

Supporting Information:

Simultaneously enhanced electrical conductivity and suppressed thermal conductivity for ALD ZnO films via purge-time controlled defects

Ramin Ghiyasi,¹ Milena Milich,² John Tomko,² Girish C. Tewari,¹ Mika Lastusaari,³ Patrick E. Hopkins² and Maarit Karppinen^{1*}

¹Department of Chemistry and Materials Science, Aalto University, FI-00076 Espoo, Finland

²University of Virginia, Department of Mechanical and Aerospace Engineering, Charlottesville, VA 22904, USA

³Department of Chemistry, University of Turku, FI-20014, Turku, Finland

*Corresponding Author: maarit.karppinen@aalto.fi

X-ray Diffraction (XRD) and Reflection (XRR) Data & Analysis

Below, XRR patterns for a series of ZnO thin films grown using different purge times, and an XRD pattern for a representative sample are shown.

The XRD patterns were collected using a PANalytical X'Pert Pro MPD Powder device with a Cu tube from 20° to 60° 2 θ .

The XRR patterns were analysed by utilization of an X'Pert Reflectivity software v1.3 from PANalytical.

XRR patterns fitting protocol

Model Construction: The starting models were constructed based on manually fitted film thickness via the Fourier transformation (FT) method and employing the density of bulk materials as starting values. From bottom to top the following layers were added: Si (as substrate), SiO₂ (1 nm), ZnO (1 nm), ZnO (FT thickness minus 2 nm), and ZnO (1 nm).

Fitting: In order to achieve the most accurate fitting the following steps were taken:

1. All the ZnO layers were linked together to be fitted as one block.
2. The silicon density was removed from fitting parameters as it is a fixed factor.
3. The segmented fitting method was selected as the fitting algorithm.
4. The fittings were initially started with a fitting range up to the last clear point of the patterns.
5. Fittings were initiated with a fitting margin of 40% for density and thickness and a margin of 0.3-4 for ZnO and SiO₂ while having 0.3-2 for Si.
6. The three groups of ZnO layers were delinked and fitted separately.
7. The full range of patterns was added.
8. Instrumental factors were added.
9. After achieving full fitting, a smaller fitting margin was selected, i.e. 20%, 10%, 5%. This procedure was stopped after achieving a full fitting at a 5% margin.
10. The obtained fittings were verified by a combined fitting method of were Genetic Algorithm and Segmented fitting method.

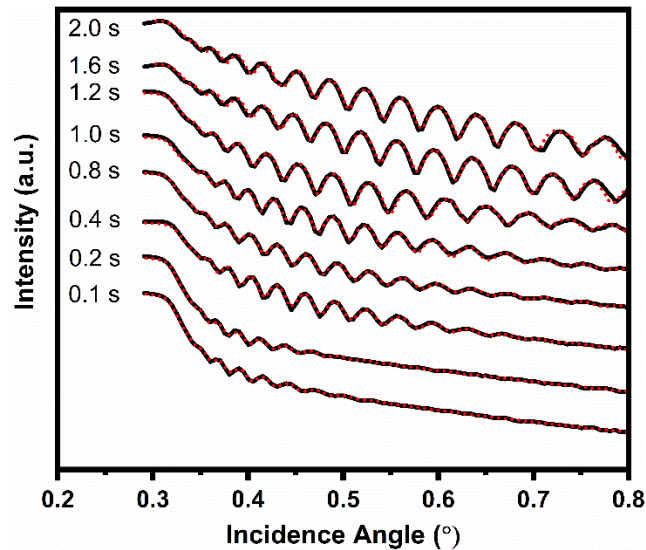


FIG. S1. Experimental (solid black lines) and fitted (dashed red lines) XRR patterns for ZnO films deposited with different N₂ purge times.

The obtained XRR patterns indicate uniform films with small fringes, which represent the reflection of the X-ray beam from layer interfaces. The effect of purge time changes on thickness and roughness are even very much clear from the patterns. The distance between the fringes is inversely proportional to the film thickness, therefore, the film thickness decreases as the purge time increases. The rate at which the signal decays is attributed to the film roughness, therefore, the roughness of the films significantly decreases as the purge time increases. Both of the aforementioned points are confirmed and measured by the fitting.

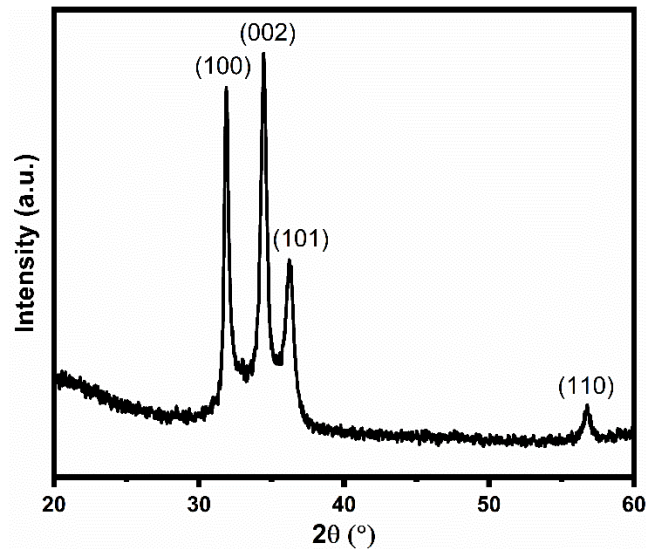


FIG. S2. X-ray diffraction pattern for a representative ZnO thin film.

The resulting XRD patterns for the obtained films fully correspond to the well-known wurtzite structure for ZnO. A sample with a pulse/purge length of 0.1/1.0 s is depicted in figure 2S as representative of all the other films. The appearance of clear peaks for (100), (002), (101), and (110) exactly at the expected degrees 31.88°, 34.46°, 36.22°, and 56.77° 2θ and no extra peaks could be taken as an indication of the purity of polycrystalline ZnO.

Thermal Conductivity Measurement Details

The reported thermal conductivity values were measured in the cross-plane direction using time-domain thermoreflectance (TDTR) measurements. This optical pump-probe technique has been widely applied to the measurement of thermal properties of thin films and structures, including our previous work on organic-inorganic SLs. In summary, a relatively high-energy ‘pump’ pulse excites the surface of the sample, while a mechanically-delayed, low-energy ‘probe’ pulse operates as an optical thermometer and monitors the transient cooling dynamics of the sample surface.¹⁻⁴ By fitting the experimental cooling curve to a multilayer thermal model over multiple modulation frequencies, we can accurately extract the thermal conductivity of the ZnO thin films. An example of our TDTR data and associated fit of the thermal model is shown in Figure S1 for ZnO deposited with a 1.2s purge time.

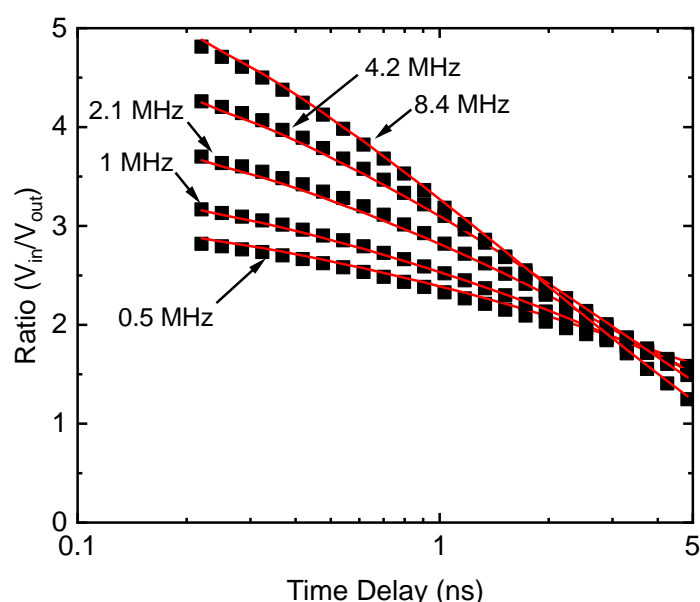


Figure S3. TDTR data using five different modulation frequencies and their associated fit for ZnO deposited with a 1.2s purge time.

We deposit an additional 80 nm Al layer on top of the thin film of interest (e.g., 80 nm Al/ZnO/sapphire substrate structure) by electron beam evaporation, which operates as an ideal thermo-optical transducer for our TDTR measurements. The reported error bars account for propagated uncertainty associated with the thermal boundary resistances of the Al/ZnO interface and ZnO/sapphire interface, as well as the laser spot size and layer thicknesses. To account for the uncertainty in the two thermal boundary resistances, we analyzed the TDTR data using an assumed “infinite” thermal boundary conductance at the ZnO/sapphire interface and fit for the resulting thermal boundary conductance at the Al/ZnO interface in addition to ZnO thermal conductivity.

Photoluminescence Measurement Details

The photoluminescence spectra were measured at room temperature using a Lotis TII Nd:YAG laser at 355 nm and operated at 19 J. On the excitation side, a Thorlabs FL355-10 filter was used, and on the emission side, a Standa BS-8 filter was used. The emission was collected with an Avantes HS-TEC CCD spectrometer using a 600-micrometer thick optical fiber.

Electrical Conductivity Measurement Details

The electrical transport properties (resistivity and Seebeck coefficient) were measured using Quantum Design Physical Property Measurement System (PPMS). The resistivity is measured by attaching four linear probes to the sample. The same probes were used to measure the Seebeck coefficient in isothermal and open-circuit condition. The carrier concentration (n) and effective mass (m^*) were calculated by the implementation of equations 1 and 2:

$$V_H = R_H \times ((I \times B)/t) \quad (\text{Eq. 1})$$

$$S = ((8\pi^2 k_B^2)/(3eh^2)) \times m^* T \times (\pi/3n) \quad (\text{Eq. 2})$$

Considering that carrier concentration (n , Eq.2) is inversely equal to Hall coefficient (R_H , Eq.1) multiplied by the electron charge (e), n can be calculated after obtaining the R_H . At each temperature, the corresponding Hall voltage (V_H , Eq.1) for the applied magnetic fields (B , Eq.1) were measured. Subsequently, by obtaining the slope of the line in V_H versus $(I \times B)/t$ (I : current, t : thickness) plot, the R_H and, as well as $1/(n \times e)$ were calculated. In Eq.2, k_B , e , h , and T , respectively denote the Boltzmann constant, electron charge, Planck constant, and temperature.^{5,6}

References

- ¹ Paddock, C. A., Eesley, G. L. Transient Thermoreflectance from Thin Metal Films. *J. Appl. Phys.* **60**, 285–290 (1986).
- ² Cahill, D. G. Analysis of Heat Flow in Layered Structures for Time-Domain Thermoreflectance. *Rev. Sci. Instrum.* **75**, 5119–5122 (2004).
- ³ Schmidt, A. J., Chen, X., Chen, G. Pulse Accumulation, Radial Heat Conduction, and Anisotropic Thermal Conductivity in Pump-Probe Transient Thermoreflectance. *Rev. Sci. Instrum.* **79**, 114902 (2008).
- ⁴ Hopkins, P. E., Serrano, J. R., Phinney, L. M., Kearney, S. P., Grasser, T. W., Harris, C. T. Criteria for Cross-Plane Dominated Thermal Transport in Multilayer Thin Film Systems During Modulated Laser Heating. *J. Heat Transfer*, 132 (2010).
- ⁵ Snyder, G. J., Toberer, E. S. Complex Thermoelectric Materials. *Nat. Mater.* **7**, 105–114 (2008).
- ⁶ Cutler, M., Leavy, J. F., Fitzpatrick, R. L. Electronic Transport in Semimetallic Cerium Sulfide. *Phys. Rev.* **133**, A1143–A1152 (1964).